

The kaobook class

**Use this document as a template**

# **My PhD Thesis**

**Customise this page according to your needs**

Tobias Hangleiter\*

March 27, 2025

\* A  $\text{\LaTeX}$  lover/hater

The harmony of the world is made manifest in Form and Number, and the heart and soul and all the poetry of Natural Philosophy are embodied in the concept of mathematical beauty.

– D'Arcy Wentworth Thompson

# Contents

<b>Contents</b>	<b>iii</b>
<b>A FLEXIBLE Python TOOL FOR FOURIER-TRANSFORM NOISE SPECTROSCOPY</b>	<b>1</b>
1 Introduction	2
2 Theory of spectral noise estimation	3
2.1 Spectrum estimation from time series . . . . .	3
2.2 Window functions . . . . .	5
2.3 Welch's method . . . . .	6
<b>CHARACTERIZATION AND IMPROVEMENTS OF A MILLIKELVIN CONFOCAL MI- CROSCOPE</b>	<b>7</b>
<b>ELECTROSTATIC TRAPPING OF EXCITONS IN SEMICONDUCTOR MEMBRANES</b>	<b>8</b>
<b>A FILTER-FUNCTION FORMALISM FOR QUANTUM OPERATIONS</b>	<b>9</b>
<b>APPENDIX</b>	<b>10</b>
<b>Bibliography</b>	<b>11</b>
<b>List of Terms</b>	<b>12</b>

**A FLEXIBLE Python TOOL FOR  
FOURIER-TRANSFORM NOISE  
SPECTROSCOPY**

Noise is ubiquitous in condensed matter physics experiments, and in mesoscopic systems in particular it can easily drown out the sought-after signal. Hence, characterizing (and subsequently mitigating) noise is an essential task for the experimentalist. But noise comes in as many different forms as there are types of signal sources and detectors, whether it be a voltage source or a photodetector, and while some instruments have built-in solutions for noise analysis, they vary in functionality and capability. Moreover, the measured signal often does not directly correspond to the noisy physical quantity of interest, making it desirable to be able to manipulate the raw data before processing.

# Theory of spectral noise estimation

# 2

There exists a multitude of methods for estimating noise properties.

lay out some others

If the noisy process  $x(t)$ <sup>1</sup> has Gaussian statistics, meaning that the value at a given point in time follows a normal distribution with some mean  $\mu$  and variance  $\sigma^2$  over multiple realizations of the process, it can be fully described by the power spectral density (PSD)  $S(\omega)$ .<sup>2</sup> For the purpose of noise estimation, the assumption of Gaussianity is a rather weak one as the noise typically arises from a large ensemble of individual fluctuators and is therefore well approximated by a Gaussian distribution by the central limit theorem.<sup>3</sup> Even if the process  $x(t)$  is not perfectly Gaussian, non-Gaussian contributions can be seen as higher-order contributions if viewed from the perspective of perturbation theory, and therefore the PSD still captures a significant part of the statistical properties. For this reason, the PSD is the central quantity of interest in noise spectroscopy and I will discuss some of its properties in the following.

1: We discuss only classical noise here, meaning  $x(t)$  commutes with itself at all times. For descriptions of and spectroscopy protocols for quantum noise refer to Refs. 1 and 2, for example.

2: The term *power spectrum* is often used interchangeably. I will do so as well, but emphasize at this point that in digital signal processing in particular, the *spectrum* is a different quantity from the *spectral density*.

maybe a classical signal processing ref?

For real signals  $x(t) \in \mathbb{R}$ ,  $S(\omega)$  is an even function and one therefore distinguishes the *two-sided* PSD  $S^{(2)}(\omega)$  defined over  $\mathbb{R}$  from the *one-sided* PSD  $S^{(1)}(\omega) = 2S^{(2)}(\omega)$  defined only over  $\mathbb{R}^+$ . Complex signals  $x(t) \in \mathbb{C}$  such as those generated by Lock-in amplifiers after demodulation in turn have asymmetric, two-sided PSDs.

3: As an example, consider electronic devices, where voltage noise arises from a large number of defects and other charge traps in oxides being populated and depopulated at certain rates  $\gamma$ . The ensemble average over these so-called two-level fluctuators (TLFs) then yields the well-known  $1/f$ -like noise spectra (at least for a large density [3]).

flesh out this sidenote?

flesh out

## 2.1 Spectrum estimation from time series

To see how the PSD may be estimated from time-series data, consider a continuous wide-sense stationary<sup>4</sup> signal in the time domain  $x(t) \in \mathbb{C}$  that is observed for some time  $T$ . We define the windowed Fourier transform of  $x(t)$  and its inverse by<sup>5</sup>

$$\hat{x}_T(\omega) = \int_0^T dt x(t) e^{-i\omega t} \quad (2.1)$$

$$\text{and } x(t) = \int_{-\infty}^{\infty} \frac{d\omega}{2\pi} \hat{x}_T(\omega) e^{i\omega t}, \quad (2.2)$$

i.e., we assume that outside of the window of observation  $x(t)$  is zero. The auto-correlation function of  $x(t)$  is given by

$$C(\tau) = \langle x(t)^* x(t + \tau) \rangle \quad (2.3)$$

$$= \lim_{T \rightarrow \infty} \frac{1}{T} \int_0^T dt x(t)^* x(t + \tau), \quad (2.4)$$

4: For a wide-sense stationary (also called weakly stationary) process  $x(t)$ , the mean is constant and the auto-correlation function  $C(t, t') = \langle x(t)^* x(t') \rangle$  is given by  $\langle x(t)^* x(t + \tau) \rangle = \langle x(0)^* x(\tau) \rangle$  with  $\tau = t' - t$ . That is, it is a function of only the time lag  $\tau$  and not the absolute point in time. For Gaussian processes as discussed here, this also implies stationarity [4]. The property further implies that  $C(\tau)$  is an even function.

sketch of auto-correlation function?

5: In this chapter we will always denote the Fourier transform of some quantity  $\xi$  using the same symbol with a hat,  $\hat{\xi}$ .

where  $\langle \cdot \rangle$  is the ensemble average over multiple realizations of the process and the last equality holds true for ergodic processes. Expressing  $x(t)$  in terms of its Fourier representation (Equation 2.1) and reordering the integrals, we get<sup>6</sup>

$$C(\tau) = \lim_{T \rightarrow \infty} \frac{1}{T} \int_0^T dt \int_{-\infty}^{\infty} \frac{d\omega}{2\pi} \hat{x}_T(\omega)^* e^{-i\omega t} \int_{-\infty}^{\infty} \frac{d\omega'}{2\pi} \hat{x}_T(\omega') e^{i\omega'(t+\tau)} \quad (2.5)$$

$$= \lim_{T \rightarrow \infty} \frac{1}{T} \int_{-\infty}^{\infty} \frac{d\omega}{2\pi} \int_{-\infty}^{\infty} \frac{d\omega'}{2\pi} \hat{x}_T(\omega)^* \hat{x}_T(\omega') e^{i\omega'\tau} \int_0^T dt e^{it(\omega' - \omega)} \quad (2.6)$$

6: Mathematicians might at this point argue the integrability of  $x(t)$ , but as we deal with physical processes with finite bandwidth (and have no shame), we do not.

The innermost integral approaches a  $\delta$ -function for large  $T$ ,<sup>7</sup> allowing us to further simplify this under the limit as

$$C(\tau) = \lim_{T \rightarrow \infty} \frac{1}{T} \int_{-\infty}^{\infty} \frac{d\omega}{2\pi} \int_{-\infty}^{\infty} \frac{d\omega'}{2\pi} \hat{x}_T(\omega)^* \hat{x}_T(\omega') e^{i\omega'\tau} \delta(\omega' - \omega) \quad (2.7)$$

$$= \lim_{T \rightarrow \infty} \frac{1}{T} \int_{-\infty}^{\infty} \frac{d\omega}{2\pi} |\hat{x}_T(\omega)|^2 e^{i\omega\tau} \quad (2.8)$$

$$= \int_{-\infty}^{\infty} \frac{d\omega}{2\pi} S(\omega) e^{i\omega\tau} \quad (2.9)$$

with the PSD

$$S(\omega) = \lim_{T \rightarrow \infty} \frac{1}{T} |\hat{x}_T(\omega)|^2 \quad (2.10)$$

$$= \int_{-\infty}^{\infty} d\tau C(\tau) e^{-i\omega\tau} \quad (2.11)$$

Equation 2.9 is the Wiener-Khinchin theorem that states that the auto-correlation function  $C(\tau)$  and the PSD  $S(\omega)$  are Fourier-transform pairs [4]. Furthermore, defining the latter through Equation 2.10 gives us an intuitive picture of the PSD if we recall Parseval's theorem,

$$\int_{-\infty}^{\infty} \frac{d\omega}{2\pi} \frac{1}{T} |\hat{x}_T(\omega)|^2 = \frac{1}{T} \int_{-\infty}^{\infty} dt |x(t)|^2. \quad (2.12)$$

That is, the total power  $P$  contained in the signal  $x(t)$  is given by integrating over the PSD. Similarly, the power contained in a band of frequencies  $[\omega_1, \omega_2]$  is given by

$$P(\omega_1, \omega_2) = \text{rms}(\omega_1, \omega_2)^2 \quad (2.13)$$

$$= \int_{\omega_1}^{\omega_2} \frac{d\omega}{2\pi} S(\omega) \quad (2.14)$$

where  $\text{rms}(\omega_1, \omega_2)$  is the root-mean-square within this frequency band. These relations are helpful when analyzing noise PSDs to gauge the relative weight of contributions from different frequency bands to the total noise power.

Equation 2.10 represents the starting point for the experimental spectrum estimation procedure. Instead of a continuous signal  $x(t)$ ,  $t \in [0, T]$ , consider its discretized version<sup>8</sup>

$$x_n, \quad n \in \{0, 1, \dots, N-1\} \quad (2.15)$$

defined at times  $t_n = n\Delta t$  with  $T = N\Delta t$  and where  $\Delta t = f_s^{-1}$  is the sampling interval (the inverse of the sampling frequency  $f_s$ ). Invoking the ergodic theorem, we can replace the long-term average in Equation 2.10 by the ensemble average over  $M$  realizations  $i$  of the noisy signal  $x_n^{(m)}$  and write

$$S_n = \frac{1}{M} \sum_{i=0}^{M-1} |\hat{x}_n^{(m)}|^2 \quad (2.16)$$

$$= \frac{1}{M} \sum_{i=0}^{M-1} S_n^{(m)} \quad (2.17)$$

where  $\hat{x}_n^{(m)}$  is the discrete Fourier transform of  $x_n^{(m)}$ , we defined the *peri-*

7: Note that, because  $x(t)$  is wide-sense stationary, we may shift the limits of integration  $\int_0^T \rightarrow \int_{-T/2}^{+T/2}$ .

8: We only discuss the problem of equally spaced samples here. Variants for spectral estimation of time series with unequal spacing exist.

ref

odogram of  $x_n^{(m)}$  by

$$S_n^{(m)} = \left| \hat{x}_n^{(m)} \right|^2, \quad (2.18)$$

and  $S_n$  is an *estimate* of the true PSD sampled at the discrete frequencies  $\omega_n = 2\pi n/T \in 2\pi \times \{-f_s/2, \dots, f_s/2\}$ .<sup>9</sup> Equation 2.16 is known as Bartlett's method [5] for spectrum estimation.<sup>10</sup>

To better understand the properties of this estimate, let us take a look at the parameters  $\Delta t$ ,  $N$ , and  $M$ . The sampling interval  $\Delta t$  defines the largest resolvable frequency by the Nyquist sampling theorem,

$$f_{\max} = \frac{f_s}{2} = \frac{1}{2\Delta t}. \quad (2.19)$$

In turn, the number of samples  $N$  determines the frequency resolution  $\Delta f$ , or smallest resolvable frequency,

$$f_{\min} = \Delta f = \frac{1}{T} = \frac{1}{N\Delta t} = \frac{f_s}{N}. \quad (2.20)$$

Lastly,  $M$  determines the variance of the set of periodograms  $\{S_n^{(m)}\}_{i=0}^{M-1}$  and hence the accuracy of the estimate  $S_n$ .

In practice, the ensemble realizations  $i$  are of course obtained sequentially, implying that one acquires a time series of data  $x_n, n \in \{0, 1, \dots, NM-1\}$  and partitions these data into  $M$  sequences of length  $N$ . It becomes clear, then, that the Bartlett average (Equation 2.16) trades spectral resolution (larger  $N$ ) for estimation accuracy (larger  $M$ ) given the finite acquisition time  $T = NM\Delta t$ .

An improvement in data efficiency can be obtained using Welch's method [6]. To see how, we first need to discuss spectral windowing.

## 2.2 Window functions

Partitioning a signal  $x_n$  into  $M$  sections  $x_n^{(m)}$  of length  $N$  is mathematically equivalent to multiplying the signal with the rectangular *window function* given by<sup>11</sup>

$$w_n^{(m)} = \begin{cases} 1 & \text{if } (m-1)N \leq n < mN \\ 0 & \text{else} \end{cases} \quad \text{and} \quad (2.21)$$

so that  $x_n^{(m)} = x_n w_n^{(m)}$ .

Now recall that multiplication and convolution are duals under the Fourier transform, implying that

$$\hat{x}_n^{(m)} = \hat{x}_n * \hat{w}_n^{(m)}. \quad (2.22)$$

where the Fourier representation of the rectangular window

$$\hat{w}_n^{(m)} = \hat{w}_n e^{-i(m-1/2)\omega_n T}, \quad (2.23)$$

$$\hat{w}_n = T \operatorname{sinc}\left(\frac{\omega_n T}{2}\right). \quad (2.24)$$

9: We blithely disregard integer algebra issues occurring here for conciseness and leave it as an exercise for the reader to figure out what the exact bounds of the set of  $\omega_n$  are.

10: By taking the limit  $M \rightarrow \infty$  one recovers the true PSD,

$$\lim_{M \rightarrow \infty} S_n = S(\omega_n).$$

The continuum limit is as always obtained by sending  $\Delta t \rightarrow 0, N \rightarrow \infty, N\Delta t = \text{const.}$

11: This window is also known as the boxcar or Dirichlet window.

add  $\omega_n^{(m)}$ , scaled ticks

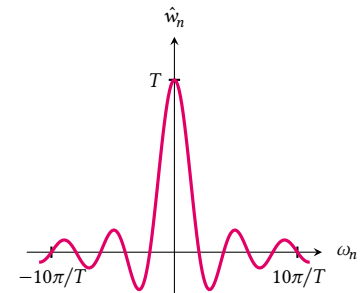


**Figure 2.1:** The Fourier representation of the rectangular window in continuous time.



Figure 2.1 shows the unshifted rectangular window  $\hat{w}_n$  in Fourier space. We can hence understand the Fourier spectrum of  $x_n^{(m)}$  as sampling  $\hat{x}_n$  with the probe  $\hat{w}_n^{(m)}$ . However, while in the continuum limit (c.f. side-note 10) Equation 2.24 tends towards  $\delta(\omega_n)$  and thus will produce a faithful reconstruction of the true spectrum, the finite frequency spacing  $\Delta f$  of discrete signals introduces a finite bandwidth of the probe as well as *sidelobes*. These effects induce what is known as *spectral leakage* [4, 7] and lead to artifacts and deviations of the spectrum estimator  $S_n$  from the true spectrum  $S(\omega_n)$ .

For this reason, a plethora of *window functions* have been introduced to mitigate the effects of spectral leakage. Key properties of a window are the spectral bandwidth (center lobe width) and sidelobe amplitude between which there typically is a tradeoff.

A window frequently used in spectral analysis is the Hann window [8],

$$w_n^{(m)} = \begin{cases} \cos^2\left(\frac{\pi n}{N}\right) & \text{if } (m-1)N \leq n < mN \text{ and} \\ 0 & \text{else} \end{cases} \quad (2.25)$$

with the Fourier representation of the unshifted window,

$$\hat{w}_n = \frac{4\pi^2}{\omega_n} \times \frac{\sin(\omega_n T/2)}{4\pi^2 - \omega_n^2 T^2}, \quad (2.26)$$

shown in Figure 2.2. The favorable properties of the Hann window are apparent when compared to the rectangular window in Figure 2.1; the sidelobes are cubically suppressed while the center lobe is only slightly broadened.

Another favorable property of the Hann window is that  $w_0^{(0)} = w_{N-1}^{(0)} = 0$ . This suppresses detrimental effects arising from a possible discontinuity ( $x_0^{(0)} \neq x_{N-1}^{(0)}$ ) at the edge of a data segment related to the discrete Fourier transform, which assumes periodic data.<sup>12</sup>

## 2.3 Welch's method

Contemplating Equation 2.25, one might come to the conclusion that using a window such as this is not very data efficient in the sense that a large fraction of samples located at the edge of the window is strongly suppressed and hence does not contribute significantly to the spectrum estimate. To alleviate this lack of efficiency, one can introduce an overlap between adjacent data windows. That is, instead of partitioning the data  $x_n$  into  $M$  non-overlapping sections of length  $N$ , one shifts the  $m$ th window forward by  $mK$  with  $K > 0$  the overlap. Finally, the periodogram (Equation 2.18) is computed for each window and subsequently averaged to obtain the spectrum estimator (Equation 2.16).

This method of spectrum estimation is known as Welch's method [6]. One can show [6] that the correlation between the periodograms of adjacent, overlapping windows is sufficiently small to avoid a biased estimate. A typical overlap is  $K = N/2$  with which one would obtain  $M = 2L/N - 1$  windows for data of length  $L$ .<sup>13</sup>

add  $\omega_n^{(m)}$ , scaled ticks

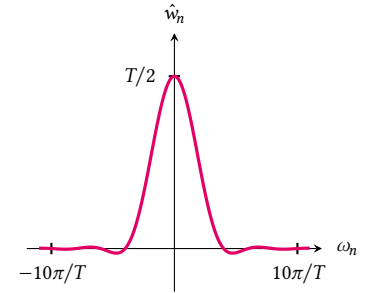


**Figure 2.2:** The Fourier representation of the Hann window in continuous time.

12: Although this can usually also be achieved by detrending the data before performing the Fourier transform, which is a good idea in any case.

13: Again neglecting integer arithmetic issues.

**CHARACTERIZATION AND  
IMPROVEMENTS OF A MILLIKELVIN  
CONFOCAL MICROSCOPE**

# **ELECTROSTATIC TRAPPING OF EXCITONS IN SEMICONDUCTOR MEMBRANES**

# **A FILTER-FUNCTION FORMALISM FOR QUANTUM OPERATIONS**

# **APPENDIX**

# Bibliography

- [1] A. A. Clerk et al. “Introduction to Quantum Noise, Measurement, and Amplification.” In: *Rev. Mod. Phys.* 82.2 (Apr. 15, 2010), pp. 1155–1208. doi: [10.1103/RevModPhys.82.1155](#). (Visited on 01/19/2022) (cited on page 3).
- [2] Gerardo A. Paz-Silva, Leigh M. Norris, and Lorenza Viola. “Multiqubit Spectroscopy of Gaussian Quantum Noise.” In: *Phys. Rev. A* 95.2 (Feb. 23, 2017), p. 022121. doi: [10.1103/PhysRevA.95.022121](#) (cited on page 3).
- [3] M. Mehmandoost and V. V. Dobrovitski. “Decoherence Induced by a Sparse Bath of Two-Level Fluctuators: Peculiar Features of 1/f Noise in High-Quality Qubits.” In: *Phys. Rev. Res.* 6.3 (Aug. 15, 2024), p. 033175. doi: [10.1103/PhysRevResearch.6.033175](#). (Visited on 08/20/2024) (cited on page 3).
- [4] Lambert Herman Koopmans. *The Spectral Analysis of Time Series*. 2nd ed. Vol. 22. Probability and Mathematical Statistics. San Diego: Academic Press, 1995 (cited on pages 3, 4, 6).
- [5] M. S. Bartlett. “Smoothing Periodograms from Time-Series with Continuous Spectra.” In: *Nature* 161.4096 (May 1948), pp. 686–687. doi: [10.1038/161686a0](#). (Visited on 03/26/2025) (cited on page 5).
- [6] P. Welch. “The Use of Fast Fourier Transform for the Estimation of Power Spectra: A Method Based on Time Averaging over Short, Modified Periodograms.” In: *IEEE Trans. Audio Electroacoustics* 15.2 (June 1967), pp. 70–73. doi: [10.1109/TAU.1967.1161901](#) (cited on pages 5, 6).
- [7] F.J. Harris. “On the Use of Windows for Harmonic Analysis with the Discrete Fourier Transform.” In: *Proc. IEEE* 66.1 (Jan. 1978), pp. 51–83. doi: [10.1109/PROC.1978.10837](#). (Visited on 03/27/2025) (cited on page 6).
- [8] A. Nuttall. “Some Windows with Very Good Sidelobe Behavior.” In: *IEEE Trans. Acoust. Speech Signal Process.* 29.1 (Feb. 1981), pp. 84–91. doi: [10.1109/TASSP.1981.1163506](#). (Visited on 03/27/2025) (cited on page 6).

# Special Terms

## P

**PSD** power spectral density. 3–5

## T

**TLF** two-level fluctuator. 3